# Contrasting response strategies of sulfate-reducing bacteria in a microbial consortium to As3+ stress under anaerobic and aerobic environments

Miaomiao Li, Jun Yao, Yating Wang, Geoffrey Sunahara, Robert Duran, Jianli Liu, Bang Liu, Houquan Liu, Bo Ma, Hao Li, et al.

# Contrasting response strategies of sulfate-reducing bacteria in a microbial consortium to $As^{3+}$ stress under anaerobic and aerobic environments

Miaomiao Li[1], Jun Yao[1,*], Yating Wang[1], Geoffrey Sunahara[1,2], Robert Duran[3], Jianli Liu[1], Bang Liu[1,3], Houquan Liu[1], Bo Ma[1], Hao Li[1], Wancheng Pang[1], Ying Cao[1]

[1] Research Center of Environmental Science and Engineering, China University of Geosciences (Beijing), 29 Xueyuan Road, Haidian District, Beijing 100083, China

[2] Department of Natural Resource Sciences, McGill University, 21111 Lakeshore Drive, Ste-Anne-de-Bellevue, Quebec, H9X 3V9, Canada

[3] Université de Pau et des Pays de l'Adour, UPPA/E2S, IPREM CNRS 5254, Pau, France

* Corresponding author:
Jun Yao (E-mail: yaojun@cugb.edu.cn)
School of Water Resource and Environment, Research Center of Environmental Science and Engineering, China University of Geosciences (Beijing), 29 Xueyuan Road, Haidian District, 100083, Beijing, China

**Abstract**

The sulfate-reducing efficiency of sulfate-reducing bacteria (SRB) is strongly influenced by the presence of oxygen, but little is known about the oxygen tolerance mechanism of SRB and the effect of oxygen on the metalliferous immobilization by SRB. The performance evaluation, identification of bioprecipitates, and microbial and metabolic process analyses were used here to investigate the $As^{3+}$ immobilization mechanisms and survival strategies of the SRB1 consortium under different oxygen-containing environments. Results indicated that the sulfate reduction efficiency was significantly decreased under aerobic (47.37%) compared with anaerobic conditions (66.72%). SEM analysis showed that under anaerobic and aerobic conditions, the morphologies of mineral particles were different, whereas XRD and XPS analyses showed that the most of $As^{3+}$ bioprecipitates under both conditions were arsenic minerals such as AsS and $As_4S_4$. The abundances of *Clostridium_sensu_stricto_1*, *Desulfovibrio*, and *Thiomonas* anaerobic bacteria were significantly higher under anaerobic than aerobic conditions, whereas the aerobic *Pseudomonas* showed an opposite trend. Network analysis revealed that *Desulfovibrio* was positively correlated with *Pseudomonas*. Metabolic process analysis confirmed that under aerobic conditions the SRB1 consortium generated additional extracellular polymeric substances (rich in functionalities such as Fe-O, S=O, C=O, and -OH) and the anti-oxidative enzyme superoxide dismutase to resist $As^{3+}$ stress and oxygen toxicity. New insights are provided here into the oxygen tolerance and detoxification mechanism of SRB and provide a basis for the future remediation of heavy metal(loid)-contaminated environments.

**Keywords:** Sulfate-reducing bacteria, Response strategies, $As^{3+}$, Anaerobic, Aerobic

## 1. Introduction

Heavy metal(loid) pollution of soil and industrial wastewater (including acid mine drainage) is a global environmental concern with the presence of more than 10 million polluted sites worldwide (Fei et al., 2019; Xiao et al., 2019; Xu et al., 2021b). It is well known that the cumulative effects of industrialization and anthropogenic activities have led to severe pollution by heavy metal(loid)s (HMs) (Chun et al., 2021) caused by the construction of mines, metal smelters, coal-fired power stations, and manufacturing factories (Yun et al., 2018; Zhang et al., 2021; Li et al., 2022a; Li et al., 2022b). Superfluous HMs entering into the environment can severely diminish soil and water quality and productivity, thereby disturbing the balance of the surrounding ecosystem, and decreasing the stability of the microbial community (Chun et al., 2021; Ran et al., 2021; Zhang et al., 2021). The release of HMs into the environment can also pose a serious health threat to humans and sensitive species of the food web (Ran et al., 2021; Li et al., 2015; Liu et al., 2017). Therefore, it is important to adopt appropriate remediation strategies for HM pollution.

Microbial strategies offer a viable and eco-friendly alternative to the stabilization of HMs using organisms such as fungi, bacteria, and plants (Sun et al., 2017; Chun et al., 2021). Biological treatment based on sulfate-reducing bacteria (SRB) is an increasingly attractive remediation strategy due to its cost-effectiveness, and ability to remove and immobilize HMs (Liu et al., 2018; Bao et al., 2020; Dev et al., 2021; Si et al., 2023). SRB is generally regarded as strict anaerobic bacteria that are widely distributed in seawater, marine sediments, hot springs, and geothermal fields, as well as in oil and gas wells (Cypionka et al., 1985; Ravenschlag et al., 2000; de Matos et al., 2018) and acid mine drainage (Giloteaux et al.,

2013), where they play an important role in the global S-cycle (Zhou and Xing, 2021; Si et al., 2023). SRB can use sulfate ($SO_4^{2-}$) as the terminal electron acceptor to generate sulfide ($S^{2-}$), which reacts with free HM ions to form insoluble metal sulfide precipitates (Liu et al., 2018; Lv et al., 2022). The role of the biomineralization process has been studied in recent years (Gu et al., 2021; Zampieri et al., 2021; Yan et al., 2023). For example, *Desulfovibrio desulfuricans* can remove Zn as zinc sulfide (ZnS) in the presence of $SO_4^{2-}$ from acid mine drainage (Hwang and Jho, 2018). Whereas an enriched SRB consortium achieved the simultaneous removal of multiple metals, including Cr, Cu, Ni, and Zn (Kieu et al., 2011). SRB can also enhance the passivation performance of biochar for immobilizing HMs (Si et al., 2023). During the application of SRB for HMs remediation, the availability of an anaerobic environment is not often assured, and SRB will face exposure to an oxygenated environment as it transits down the soil column. From the initial aerobic layer, and the SRB gradually penetrates down to the anoxic layer interface and finally reaches the anaerobic layer interface at a certain depth. Therefore, for practical purposes, the survival of SRB in oxygen-containing environments must be elaborated. To the best of our knowledge, most peer-reviewed SRB studies have been conducted in anaerobic environments. The immobilization of HMs by SRB under aerobic conditions has rarely been reported. Therefore, this knowledge gap regarding the effect of oxygen on the metalliferous immobilization by SRB should be investigated.

The fermentation efficiency of an anaerobic system could be facilitated by a small amount of oxygen (Nguyen et al., 2019), which enhances the diversity and activity of facultative bacteria to maintain the activity of oxygen-sensitive anaerobic bacteria. The

presence of oxygen may create a niche for specific bacteria in an anaerobic consortium to facilitate biological metabolic processes, such as the methanogen and organohalide-respiring bacteria (Chen et al., 2023). Furthermore, the oxygen tolerance of anaerobic bacteria could be due to the consumption of oxygen by co-existing aerobic bacteria or that aerobic bacteria protect anaerobic bacteria from oxygen exposure (Dalsgaard et al., 2014; Oshiki et al., 2016; Yue et al., 2018; Okabe et al., 2023). These studies indicate that anaerobic bacteria can survive under aerobic conditions and possess oxygen tolerance, thereby providing support for the aerobic survival of SRB (Fourçans et al., 2007). However, relatively little is known about the survival strategies of SRB in oxygen-containing environments.

The sulfate-reducing consortium, SRB1, which was obtained in a previous study (Li et al., 2022b), can still immobilize $As^{3+}$ and retain sulfate-reducing function in the tailings remediation process (under aerobic conditions), and suggests that SRB1 can tolerate a certain concentration of oxygen. Therefore, the objectives of the present study are (1) to compare the differences in the immobilization mechanism of $As^{3+}$ by an SRB1 consortium under anaerobic and aerobic conditions and (2) to reveal the survival strategies of SRB in the SRB1 consortium under oxygen-containing conditions from a molecular perspective.

## 2. Materials and methods

### 2.1 Chemicals, reagents, and culture media

Analytical grade sodium arsenite ($NaAsO_2$, CAS 7784-46-5) was purchased from Beijing Inokay Technology (China). The standard reference material GSB 04-1767-2004 (obtained from the National Center of Analysis and Testing for Nonferrous Metals and

Electronic Materials, China) confirmed the analytical quality of arsenic determinations. Information on medium A is detailed in Supplementary Text S1. All other chemicals used in this study were obtained from commercial sources and were at least of analytical grade purity.

### 2.2 Biosystem setup and operational conditions

The SRB1 microbial consortium was obtained from Huilong nonferrous metal smelter soil, which was heavily contaminated with arsenic (Li et al., 2022b). The SRB1 microbial consortium was cultured in medium A. Batch experiments were performed by adding $NaAsO_2$ stock solution (2000 mg/L) to medium A to achieve an initial concentration of 50 mg $As^{3+}$ /L. This concentration was selected because the SRB1 consortium can function well at 50 mg $As^{3+}$ /L (Li et al., 2022b).

All batch experiments were performed using 250 mL serum bottles filled with approximately 200 mL medium A and sterilized by autoclaving at 121℃ for 25 min and protected against light by aluminum foil to minimize photo-oxidation of $As^{3+}$. The experimental group (nine serum bottles) was inoculated with SRB1 microbial consortium and was treated under anaerobic, anoxic, and aerobic conditions, whereas the abiotic controls (nine serum bottles) received the same treatments but did not contain added inoculum. The anaerobic experiments were degassed using bubbled pure $N_2$ for 10 min and sealed with rubber plugs. The anoxic experiments were sealed using an airtight cap, and the aerobic experiments were sealed with an air-porous membrane. The initial dissolved oxygen (DO) concentrations under three conditions were measured by a DO meter (PreSens Fibox 4 trace, Germany). Sample aliquots were taken daily, and the biomass and solid samples were taken

and harvested by centrifugation at 8000 rpm for 10 min at specific time points (0, 2, 5, and 7 d) under anaerobic, anoxic, and aerobic conditions for the microbial and mineralogical analyses. All treatments were performed in triplicate and incubated at 30℃ for 7 d.

## 2.3 Immobilization of $As^{3+}$ studies

### 2.3.1 Aqueous speciation analysis

The microbial culture sample was centrifuged and then the supernatant was passed through a 0.22-μm filter to facilitate subsequent analysis. The pH, ORP, biomass of bacterial culture ($OD_{600}$), and the concentrations of total As, $SO_4^{2-}$, and $S^{2-}$ were determined in the samples (details in Supplementary Text S2).

### 2.3.2 Solid phase analysis

The samples collected under the studied conditions during specific periods were centrifuged before being washed with ultrapure water and freeze-dried for 24 h. These samples were sent to Beijing Weizhen Technology (China) for further analysis. Detailed information is provided in Supplementary Text S2.

## 2.4 Microbial analysis

The analyses of microbial communities of the collected SRB1 consortium exposed to 50 mg $As^{3+}$/L were carried out at 0, 2, 5, and 7 d under anaerobic, anoxic, and aerobic culture conditions. The details of total genomic DNA extraction are described in Supplementary Text S3. The raw sequence data of the bacterial community obtained in this study was submitted to the NCBI database (Accession No. PRJNA983256). The microbial extracellular polymeric substances (EPS) consisting of extracellular protein (PN), polysaccharide (PS), and

153 humic-like substances (HS) were also determined and quantified at 2, 5, and 7 d under the
154 studied incubation conditions. Moreover, it is generally accepted that reactive oxygen species
155 (ROS) can be produced after molecular oxygen enters the cells. Being potent oxidants ROS
156 can damage DNA and proteins (Morris, 1975; Okabe et al., 2023). Microorganisms can
157 secrete anti-oxidative enzymes to detoxify ROS and adapt to excess oxygen (Jenney et al.,
158 1999). Catalase (CAT), superoxide dismutase (SOD), and peroxidase (POD) activities were
159 determined at day 7, according to Okabe et al (2023), as described in Supplementary Text S4.

160 2.5 Statistical analysis

161 The relative abundance, heatmap, and co-occurrence patterns were plotted using
162 commercial software (as described in Supplementary Text S5). Spearman's correlation
163 coefficient analysis ($R > |0.7|$ and $P < 0.05$) was calculated to confirm the biological
164 interactions. Statistically significant differences between different groups at $P < 0.05$ were
165 carried out by the one-way analysis of variance (ANOVA) using SPSS software (ver.18.0).
166 Data was expressed as mean ± SD (standard deviation) (n = 3).

167 **3. Results and discussion**

168 3.1 Performance of SRB1 consortium on $As^{3+}$ immobilization

169 Using an initial $As^{3+}$ concentration of 50 mg/L, the performance of the SRB1 consortium
170 was determined under anaerobic, anoxic, and aerobic conditions. There were significant
171 differences in DO under anaerobic, anoxic and aerobic conditions, which reached 3.05±0.14
172 mg/L, 5.62 ± 0.21 mg/L and 6.35 ± 0.12 mg/L, respectively ($P < 0.05$, Fig. S1). The pH of
173 the SRB1 consortium decreased initially on day 1 (from pH 5.58-5.68 to pH 5.44-5.49) under

the three conditions, and then increased from day 2 to day 7 (Fig. 1A). There was no difference in pH between anaerobic and anoxic conditions ($P > 0.05$), and the pH increased slightly from pH 5.58-5.68 to ~ pH 6.0 on day 7. It was noteworthy that the pH increased by 35.71% from the initial pH 5.6 ± 0.1 to pH 7.6 ± 0.1 on day 7 ($P < 0.05$) under the aerobic conditions, which was higher than those under anaerobic or anoxic conditions. This increase in pH was likely attributed to $HCO_3^-$ (in the system) that consumes $H^+$ to increase the pH (Liu et al., 2018). In contrast, the pH of the control group remained stable at approximately pH 4.5.

There were significant differences among the ORP variation of the SRB1 consortium ($P < 0.05$) under the three conditions (Fig.1A). The initial ORP was maintained below zero, likely due to the initial addition of the inoculated microbial consortium. The ORP varied similarly under the anaerobic and anoxic conditions ($P > 0.05$), decreasing slowly from day 1 (-20 ± 14.7 mV) to day 7 (-8 ± 10.7 mV). Under aerobic conditions, the ORP decreased sharply from day 1 to day 2, and subsequently remained stable, from an initial value of -38 ± 10 mV and reached about -127 ± 8.7 mV on day 7. The pH and ORP are important environmental factors for the function of microorganisms (Jin and Kirk, 2018). The present results indicate that the pH and ORP under aerobic conditions were different compared to those under anaerobic and anoxic conditions and suggest that aerobic conditions provide a favorable habitat for SRB1.

The density of plankton biomass (at $OD_{600}$) under the different culture conditions is shown in Fig. 1B. Under anaerobic conditions, the plankton biomass gradually increased and reached 2.4 ± 0.1 on day 7. Under anoxic conditions, the plankton biomass increased slowly

196 from day 0 to day 4, entered a plateau period, and then began to decline after day 5, reaching
197 an $OD_{600}$ of 1.4 ± 0.1 on day 7. Under aerobic conditions, the plankton biomass increased
198 sharply from the initial $OD_{600}$ of 0.8 ± 0.1 to 3.2 ± 0.1 during 7 d of operation, which was
199 higher than that under anaerobic and anoxic conditions ($P < 0.05$), indicating that aerobic
200 conditions were more conducive to the growth of SRB1 microorganisms.

201 The decrease in the total As concentration in the aqueous phase was noticeable during
202 the first three days of the study (Fig. 1B). Under anaerobic conditions, the total As
203 concentration (mg/L) continued to decrease after day 3, from the initial value of 54.7 ± 1.1 to
204 6.5 ± 1.6 on day 7. Under anoxic conditions, the total As concentration decreased during the 4
205 d of incubation, from the initial 54.6 ± 1.2 to 9.1 ± 0.6 on day 4 and then increased to 10.1 ±
206 0.9 on day 7. Interestingly, the total As concentration gradually increased under aerobic
207 conditions from 11.1 ± 0.6 on day 3 to 21.1 ± 1.9 on day 7, which was higher than that under
208 anaerobic (6.5 ± 1.6) or anoxic conditions (10.1 ± 0.9) on day 7. This difference was probably
209 related to the oxidation of As-containing minerals in the aerobic water environment
210 suggesting that aerobic and anoxic conditions do not favor $As^{3+}$ immobilization by SRB.

211 To investigate the performance of the SRB1 consortium on sulfate reduction under
212 anaerobic, anoxic, and aerobic conditions, the dynamic changes of $SO_4^{2-}$ and $S^{2-}$
213 concentrations were determined. The concentration of $SO_4^{2-}$ (mg/L) decreased from the
214 initial 691.2 ± 4.3 and 722.3 ± 2.0 to 230.0 ± 10.1 and 406.5 ± 6.9 during the 7 d of operation
215 ($P < 0.05$), under anaerobic and aerobic conditions, respectively (Fig. 1C). However, the
216 $SO_4^{2-}$ concentration decreased narrowly under anoxic conditions, and the $SO_4^{2-}$ reduction
217 efficiency was only 10.3% during operation. On the other hand, the production of $S^{2-}$ under

anoxic conditions was much lower than that observed under either anaerobic or aerobic conditions (Fig. 1C), which coincided with the dynamic changes of $SO_4^{2-}$. The dynamic changes of biomass and total As concentration, along with the reduction of $SO_4^{2-}$ and the production of $S^{2-}$imply that the behavior of the SRB consortium under aerobic conditions differs compared to under anaerobic conditions. This observation suggests that the growth of SRB1 microorganisms is favored under aerobic conditions which is in contrast to the immobilization of $As^{3+}$ and the reduction of $SO_4^{2-}$ that are favored under anaerobic conditions.

### 3.2 Identification of bioprecipitates under varied conditions

The SEM, XRD, and XPS analyses were used to investigate the transformation process of SRB1 consortium solid phase morphology for different durations under the three studied conditions. In SEM images (Fig. 2), the morphology of mineral particles was similar on day 2, exhibiting multiple columnar clusters irrespective of the incubation condition. However, after day 5, these mineral particles displayed an inconsistent appearance between the anaerobic and aerobic conditions. Under anaerobic conditions, the solids took a smooth blanket-like structure on day 5, despite the presence of nano-sized particles on the surface; transformation into tight columnar clusters was seen on day 7. Compared to anaerobic conditions, many nano-sized surficial particle layers were more dispersed and distributed from days 5 to 7 under aerobic conditions. The morphology of the solid phase under anoxic conditions was similar to those found in the middle of aerobic and anaerobic exposures, with many aggregates forming by day 5, and then converted to a porous flake-like cluster on day 7.

The XRD analysis showed that the main components of bioprecipitates were similar

under anaerobic and aerobic conditions (Fig. 3). During incubation, the indicative diffraction peaks of AsS and $As_4S_4$ were detected, and the sharp peaks appeared at $2\theta = 13.231°$ on day 7, which indicates the presence of arsenolamprite (As). Uniquely, the ferrisymplesite ($Fe_3(AsO_4)_2 \cdot 6H_2O$) appeared on day 7 under aerobic conditions. Thus, the XRD patterns suggest that the main formation of bioprecipitates was weakly associated with anaerobic and aerobic conditions during the short term and that aerobic conditions did not affect the sulfate-reducing activity of the SRB1 consortium.

Further investigations using XPS analysis were performed to infer the formation and composition of bioprecipitates, with a focus on determining the chemical species of As, Fe, and S. The XPS spectrum related to As-3d was mainly divided into three particular peaks (eV) at 41.28, 42.96, and 44.78, which were assigned to As(-I)-S, As(III)-S, and As(III)-O, respectively. On day 7, the As-3d was similar under anaerobic and anoxic conditions (Fig. 4), existing mainly as As(III)-S and As(III)-O. The additional As(-I)-S components were detected in aerobic conditions only. Such observation suggested that the surficial arsenic-containing sulfide minerals were oxidized before day 7 (Fig. 1B), consistent with the previous studies (Feng et al., 2021; Chen et al., 2022).

The S *2p* signals in XPS spectra contained mainly five peaks (eV) at approximately 163.08, 164.68, 168.69, and 170.28, corresponding to $S_2^{2-}$, $S^0$, $SO_4^{2-}$, and $S_2O_3^{2-}$, respectively. The $S_2^{2-}$ had a higher content (%) under aerobic conditions (66.23) than under anaerobic (54.35) and anoxic (24.74) conditions. Correspondingly, the $SO_4^{2-}$ had a lower content under the aerobic (11.92) than under the anaerobic (33.69) or anoxic (52.63) conditions. These results suggested that the biological reduction of $SO_4^{2-}$ under anoxic conditions was much

slower than that under the anaerobic and aerobic conditions, which coincided with the previous changes of $SO_4^{2-}$ concentration (Fig. 1C). Moreover, many intermediate-valent S products were detected in the process of $SO_4^{2-}$ reduction, such as $S_2O_3^{2-}$, $S^0$, and $SO_3^{2-}$ (Fig. 4).

The XPS spectra of Fe *2p* were also analyzed and fitted with many peaks (eV), including $Fe^{2+}$ signals at 710. 92 and 725.18, $Fe^0$ signals at 719. 28 and 720.68, and different $Fe^{3+}$ signals at 712.88, 715.98, 717.08, 726.68, 728.58, and 729.48. $Fe^{2+}$ is the chemical state of Fe-oxide and sulfide species, and $Fe^{3+}$ is the oxidized state (Xu and Fu, 2022). Under aerobic and anoxic conditions, the integrated peak area of $Fe^{3+}$ was higher than that under anaerobic conditions, indicating that the iron oxidation was more intense under aerobic and anoxic conditions. Therefore, although there are differences in the changes of As, Fe, and S species under anaerobic and aerobic conditions, the SRB1 consortium can generally achieve sulfate reduction and immobilize As in the form of arsenic minerals (AsS and $As_4S_4$) under anaerobic and aerobic conditions. Moreover, Fe likely plays an important role in the process of As detoxification.

### 3.3 Dynamics of microbial community structure

The microbial diversity of the SRB1 consortium incubated under the three studied conditions was characterized through the 16S rRNA gene sequencing to identify the interactions between microorganisms in samples taken at days 0, 2, 5, and 7. After de-multiplexing and removing chimeras, a total of 936,663 valid reads were obtained from 12 samples of the SRB1 consortium, which were clustered into 410 operational taxonomic units (OTUs) according to the sequence similarity of 97%. The sequencing coverage of all samples

was > 0.99, indicating that the constructed reads library was sufficiently reliable for further analysis. Regardless of the conditions, the OTUs and Chao1 values gradually declined in the first five days and increased subsequently (Table S1). The Shannon index significantly increased after two days compared with the initial value, whereas the opposite trend was observed in the Simpson index. These results showed that under arsenic stress, the microbial community richness and diversity of the SRB1 consortium displayed a significant difference during the experiment.

The microbial population structure of the SRB1 consortium under the three studied conditions at the phylum level was altered significantly during sulfate reduction (Fig. S2). Pseudomonadota is predominant in the initial community of the SRB1 consortium with a relative proportion > 90.0%, decreased subsequently throughout the prolonged incubation in all three conditions. In contrast, Bacillota was enriched after two days, and the relative proportions (%) of Bacillota under anaerobic (43.8 - 45.0) and anoxic conditions (41.7 - 49.4) were higher than that obtained under aerobic conditions (15.4 - 37.4) ($P < 0.05$). Bacteroidota was also slightly enriched after five days, with the relative proportions of 5.6 -7.7 (anaerobic) and 5.2 -6.4 (aerobic), respectively, whereas no obvious difference was seen under anoxic conditions.

The top 15 predominant genera were identified (Fig. 5A). The taxa affiliated with *unclassified_f_Enterobacteriaceae*, *Clostridium_sensu_stricto_1,* and *Pseudomonas* were the most abundant genera, accounting for > 70% of the whole microbial sequences. The microbial diversity and structures of the SRB1 consortium at the genus level were significantly distinct under aerobic, anaerobic, and anoxic conditions (Fig. 5B). Compared to

306 the inoculum, the relative proportions of *Clostridium_sensu_stricto_1* and *Anaerocolumna*
307 showed a significant upward trend with the ongoing sulfate reduction. The relative
308 proportions (%) of *unclassified_f_Enterobacteriaceae* decreased greatly under anaerobic
309 (from 69.9 to 41.6), anoxic (from 67.3 to 40.6), and aerobic (74.5 to 16.0) conditions.

310 The relative proportions of the taxa affiliated with the anaerobic bacteria
311 *Clostridium_sensu_stricto_1*, *Anaerocolumna*, *Desulfovibrio,* and *Thiomonas* were higher
312 under anaerobic and anoxic conditions than under aerobic conditions ($P < 0.05$). In the
313 present study, the relative abundances (%) of *Clostridium_sensu_stricto_1* under anaerobic,
314 anoxic, and aerobic conditions were 31.0, 31.4, and 11.3, respectively.
315 *Clostridium_sensu_stricto_1* is affiliated with iron-reducing members and usually has high
316 relative abundances during changing redox conditions. *Anaerocolumna* was determined on
317 day 7 under aerobic conditions with an abundance of 0.4%, while its abundance under the
318 anaerobic and anoxic conditions reached 0.7% and 0.9%, respectively. *Anaerocolumna* (an
319 anaerobic bacteria) is widely found in the anaerobic digestive system and has a relatively
320 superior environmental resistance (Xu et al., 2021a). *Thiomonas* belongs to the facultative
321 chemolithoautotrophs and has a growth preference for a mixed nutrient medium containing
322 reducing inorganic S compounds and organic matter (Jia et al., 2022).

323 *Desulfovibrio*, a typical SRB widely present in anaerobic and anaerobic environments
324 (Zhou et al., 2014; Li et al., 2022c) was detected on day 5 under anaerobic, anoxic, and
325 aerobic conditions with an abundance (%) of 0.7, 0.9, and 0.2, respectively. In the present
326 study, the relative abundance of *Desulfovibrio* under aerobic conditions was significantly
327 lower than that under anaerobic or anoxic conditions. This implies that the abundance of

328 *Desulfovibrio* was positively and proportionally related to the oxygen concentration, which is
329 consistent with the normal survival law of anaerobic bacteria. Moreover, the presence of
330 *Desulfovibrio* under aerobic conditions also suggests that it can tolerate oxygen concentration
331 within a certain range.

332 The taxa affiliated with *Pseudomonas* showed an opposite trend, being detected on day 7
333 with a relative abundance (%) of 1.2, 13.2, and 57.4 under anaerobic, anoxic, and aerobic
334 conditions, respectively. Members of the *Pseudomonas* genera, gram-negative obligate
335 aerobe, can grow using different anaerobic mechanisms (Jia et al., 2022). For example,
336 *Pseudomonas* can change the hydrophobicity of its cell wall by adjusting the composition of
337 the cell membrane lipopolysaccharide, thus enhancing the interactions with other substances
338 (Rogers et al., 2020).

339 It is worth noting that the SRB1 bacteria can retain its sulfate-reducing activity under
340 aerobic conditions (Fig. 1C), indicating that sulfate-reducing bacteria (*Desulfovibrio*) can
341 survive and stay functional under aerobic conditions. Although SRBs are traditionally
342 considered strictly anaerobic, many studies have consistently observed aerobic survival and
343 oxygen resistance (Fournier et al., 2004; Ramel et al., 2013; Ramel et al., 2015; Chen and
344 Zhang, 2019). Certain SRB species can survive temporarily when exposed to oxygen
345 (Cypionka et al., 1985). *Desulfovibrio* is a relatively common class of SRB that plays a major
346 role in the S cycle (Chen and Zhang, 2019; Nagar et al., 2022). Risatti et al. (1994) analyzed
347 the microbial communities of cyanobacteria from saline-evaporated ponds and found that the
348 *Desulfovibrio* population was overwhelmingly dominant in oxygenated areas with light. In
349 addition, the co-culture experiments have shown that coexisting bacteria can consume oxygen

in the environment to aid *Desulfovibrio* survival in a high-oxygen environment (Sigalevich et al., 2000; Vita et al., 2008). Therefore, the observation reported here is not only related to the adaptation strategy of *Desulfovibrio* in an aerobic environment but also reflects the beneficial contribution of co-existing bacteria (possibly the aerobes, e.g., *Pseudomonas*) in the SRB1 consortium, which would increase *Desulfovibrio* oxygen tolerance by consuming the oxygen in the environment (Sigalevich et al., 2000; Chen and Zhang, 2019).

### 3.4 Co-occurrence patterns of bacterial communities and metabolic process variation

To further study the bacterial interactions in the SRB1 consortium, the microbial co-occurrence patterns were constructed by the strong correlations (Spearman $R > |0.7|$) and significant differences ($P < 0.05$) to filter the OTUs (Fig. 6A). The networks of the SRB1 consortium consisted of 206 nodes and 549 edges (Table S2). Pseudomonadota (34.95%) and Bacillota (16.02%) affiliated phylotypes dominated the networks, followed by Actinomycetota (11.17%), norank_k_Bacteria (10.68%), Acidobacteriota (8.25%), Bacteroidota (7.77%), Gemmatimonadetes (3.4%), and Chloroflexi (1.94%).

Interestingly, 99% of edges were positively correlated, indicating that the microorganisms in the SRB1 consortium could cooperate in response to arsenic and oxygen stress. To investigate the hypothesis that symbiotic aerobic bacteria (*Pseudomonas*) in the SRB1 consortium consume environmental oxygen to provide a niche for SRB (e.g., *Desulfovibrio*), the co-cultures were used to determine the species cooperation network at the genus level (Fig. 6B). The screening condition was kept to only the genera whose sum of relative abundance was > 0.005%, and the filtered OTUs simultaneously appeared in five samples. Spearman's correlation coefficient analysis ($R > |0.7|$ and $P < 0.05$) was then carried

out to investigate the interactions with each of the two genera (Li et al., 2023). These results provide further evidence that the taxa affiliated with *Pseudomonas* had a positive cooperative relationship with *Desulfovibrio* (Table S3). In future studies, pure strains of *Desulfovibrio* and *Pseudomonas* genera should be screened from the SRB1 consortium, and the interactions of a synthetic microbial community could be studied to further determine the survival strategy of SRB under oxygen-containing conditions.

Moreover, extracellular polymeric substances (EPS) produced by SRB play an important role in immobilizing HMs in the environment (Liu et al., 2021). Exposure to HMs could induce microorganisms to generate EPS, forming complexes with metals as a defense mechanism (Wang et al., 2014). The EPS includes proteins (PN), polysaccharides (PS), humic substances (HS), and nucleic acids, among which proteins are a dominant component affecting the fate of HMs (More et al., 2014; Yan et al., 2020). Therefore, the EPS fraction of the SRB1 consortium was determined under anaerobic, anoxic, and aerobic conditions. Data indicated that PN was the main EPS, followed by HS, and a small quantity of PS (Fig. 6C). It is worth noting that these EPS components decreased progressively during incubation, which was inseparable from the decrease in As concentrations because the production of EPS by microorganisms was not needed for the As stress resistance (Wang et al., 2014). In addition, the PN produced by the SRB1 consortium on day 2 under aerobic conditions was significantly higher than under the other two conditions, which may be related to the response of SRB to oxygen stress under aerobic conditions.

The FTIR analysis was used to determine the changes of functional groups on the EPS fraction under the different incubation conditions (Zhao et al., 2023). No obvious shifts

occurred, as evidenced by the main absorption bands ($cm^{-1}$) (Fig. 6D) appearing at about 618 (Fe-O), 1108 (S=O), 1655 (C=O), and 3291 (-OH) in the FTIR spectrum of EPS (Barakan et al., 2019; Feng et al., 2019; Zhang et al., 2019). Multifarious functional groups such as -COOH, C-N, and C-H (Shi et al., 2020; Wang et al., 2021; Wu et al., 2023) were also detected in the EPS. The -OH and -COOH were the key functional groups in the EPS of the cell surfaces, which are relevant to PN and HS or PS (Wu et al., 2023), likely providing potential binding sites for the exchange or complexation with $As^{3+}$ (Zhao et al., 2023).

Additionally, the CAT, POD, and SOD activities of the SRB1 consortium were determined under the three studied conditions on day 7 (Fig. S3). The results show that the SRB1 consortium exhibited higher SOD activities (U/mL) under aerobic conditions (15.58) than under anaerobic and anoxic conditions (both ranging from 2.57 to 3.58). The CAT and POD antioxidant enzymes of the SRB1 consortium possessed low activities under all exposure conditions, consistent with an earlier report (Okabe et al., 2023). The SOD activities of aerobic and facultative bacteria were between 10.9 and 49.7, and the normal SOD activity of aero-tolerant anaerobic bacteria was from 0.44 to 19.6 (Tally et al., 1977; Rolfe et al., 1978). Therefore, the high SOD activity level of the SRB1 consortium under aerobic conditions can further explain the survival of SRB in an oxygen-containing environment.

### 3.5 Possible survival mechanisms and environmental implications

A model of $As^{3+}$ immobilization and survival strategy by the SRB1 consortium under aerobic conditions is proposed in Fig. 7. Under aerobic conditions, the SRB1 consortium retained the ability to reduce $SO_4^{2-}$ and immobilize $As^{3+}$ into arsenic sulfides ($As_4S_4$ and AsS), which was consistent with our previous findings of products under anaerobic conditions (Li

et al., 2022b). However, redissolution of arsenic likely occurs at a later stage under aerobic conditions. Additionally, the abundance of *Desulfovibrio* clearly decreased under aerobic conditions, whereas the aerobic *Pseudomonas* was significantly enriched. Bacterial interaction analysis demonstrates a positive correlation between *Desulfovibrio* and *Pseudomonas*. The enriched strains of *Pseudomonas* likely consume more oxygen, which would create a niche for the *Desulfovibrio* in the SRB1 consortium (Chen et al., 2023). It seems reasonable that the SRB1 consortium produces additional EPS (PN) and exhibited high antioxidative enzyme activity such as SOD to reduce ROS toxicity and survive in the presence of excess oxygen.

Therefore, the survival of SRB in oxygen-containing environments may be related to the contribution of coexisting (mutualistic-symbiotic) bacteria providing a niche for *Desulfovibrio* by consuming oxygen in the environment and increasing their oxygen tolerance levels, as well as enabling the SRB to generate EPS and SOD as additional adaptation strategies. The complex mechanisms involved in the contribution of these co-existing bacteria to engender *Desulfovibrio* oxygen resistance under aerobic conditions were not confirmed here using pure strains. Future studies are planned to use metagenomics to uncover the underlying mechanisms of oxidative stress of the SRB1 consortium in an oxygen-containing water environment, as well as to identify the effects of oxygen on SRB1 incubated in actual environmental media (soil and water samples). It is anticipated that these studies will stimulate the interest of researchers and environmental engineers to utilize SRB as a remediation tool to treat HM-contaminated wastewater or tailings. The present study furthers the awareness of traditional anaerobic SRB and provides a deeper understanding of

438 the biogeochemical behavior of SRB for future studies in the laboratory or field.

## 439 4. Conclusion

440 SRBs are generally regarded as strict anaerobic bacteria, which play a potential role in
441 the bioremediation of nonferrous metal-contaminated environments, but little is known about
442 the oxygen tolerance mechanism of SRB and the effect of oxygen on the metalliferous
443 immobilization by SRB. In the present study, the immobilization mechanism of the SRB1
444 consortium on $As^{3+}$ under anaerobic and aerobic conditions was compared, as well as the
445 survival strategy of SRB1 under oxygen-containing conditions was illustrated. The studied
446 enriched sulfate-reducing consortium (SRB1) can generate additional EPS and SOD which
447 were rich in functionalities such as Fe-O, S=O, C=O, and -OH under aerobic conditions to
448 resist $As^{3+}$ stress and oxygen toxicity. Such functional groups could potentially scavenge
449 oxygen and also act as binding sites for $As^{3+}$ leading to its immobilization under aerobic
450 conditions. In contrast, this consortium showed similar $As^{3+}$ immobilization activities under
451 both conditions, such as the formation of $As^{3+}$ bioprecipitates under both conditions, mainly
452 arsenic minerals (AsS and $As_4S_4$) identified by XRD and XPS analysis. The anaerobic
453 *Desulfovibrio* was positively correlated with aerobic *Pseudomonas* suggesting the potential
454 symbiotic strategy to adapt to $As^{3+}$ stress. We posit that the survival strategy of *Desulfovibrio*
455 in the SRB1 consortium under aerobic conditions is attributed to co-existing bacteria that
456 consume oxygen, providing a niche for *Desulfovibrio* and thus improving its tolerance to
457 oxygen. On the other hand, another adaptation strategy of *Desulfovibrio* to the aerobic
458 environment is the production of additional EPS and SOD. To our knowledge, this is the first
459 report on the immobilization and survival strategy of SRB for $As^{3+}$ under aerobic conditions.

This study presents new insights into the oxygen tolerance and detoxification mechanism of SRB and provides a basis for future engineering applications of SRB as a remediation tool.

**Acknowledgments**

This work has been supported partly by grants received from the Major National R & D Projects from the Chinese Ministry of Science and Technology (2019YFC1803500, 2021YFE0106600), the National Science Foundation of China (42230716), the 111 Project (B21017) and the 1000-Talents Plan Project (WQ2017110423). We thank Dr. Jihai Gu (Hebei University) and Professor Jalal Hawari (Ecole Polytechnique de Montréal) for their comments and review of an earlier version of this manuscript.

**Author contributions**

**Miaomiao Li and Yating Wang:** Conceptualization, Methodology, Resources, Formal analysis, Writing - original draft, Writing – review & editing. **Jun Yao:** Writing – review & editing, Funding acquisition. **Geoffrey Sunahara and Bang Liu:** Conceptualization, Data Curation, Visualization, Writing – review & editing. **Jianli Liu, Houquan Liu, Bo Ma, Hao Li, Wancheng Pang and Ying Cao:** Writing – review & editing.

## References


Bao, Y.P., Jin, X.H., Guo, C.L., Lu, G.N., Dang, Z., 2020. Sulfate-reducing bacterial community shifts in response to acid mine drainage in the sediment of the Hengshi watershed, South China. Environ. Sci. Pollut. Res. 28(3), 2822-2834. doi: 10.1007/s11356-020-10248-7

Barakan, S., Aghazadeh, V., Samiee Beyragh, A., Mohammadi, S., 2019. Thermodynamic, kinetic and equilibrium isotherm studies of As(V) adsorption by Fe(III)-impregnated bentonite. Environ. Dev. Sustain. 22(6), 5273-5295. doi: 10.1007/s10668-019-00424-2

Chen, M.J., Zhang, Z.F., Hu, X.J., Tian, J.P., Lu, Z.Y., Wang, J.S., Wan, R.D., Zhou, X., Zhou, X.J., Shen, P.L., Liu, D.W., 2022. Oxidation mechanism of arsenopyrite under alkaline conditions: Experimental and theoretical analyses. J. Clean. Prod. 358. doi: 10.1016/j.jclepro.2022.131987

Chen, W.Y., Wu, J.H., Wang, B.N., 2023. Intermittent oxygen supply facilitates codegradation of trichloroethene and toluene by anaerobic consortia. Environ. Sci. Technol. 57(28), 10252-10262. doi: 10.1021/acs.est.3c02481

Chen, Y.W., Zhang, Z.H., 2019. Oxygen tolerance of sulfate reducing bacteria in fresh and coastal sea waters under enrichment culture conditions. Geological Journal of China Universities. 25(5), 705-713. doi: 10.16108/j.issn1006-7493.2019025

Chun, S.J., Kim, Y.J., Cui, Y.S., Nam, K.H., 2021. Ecological network analysis reveals distinctive microbial modules associated with heavy metal contamination of abandoned mine soils in Korea. Environ. Pollut. 289, 117851. doi: 10.1016/j.envpol.2021.117851

Cypionka, H., Widdel, F., Pfennig, N., 1985. Survival of sulfate-reducing bacteria after oxygen stress, and growth in sulfate-free oxygen-sulfide gradients. FEMS Microbiol. Lett. 31(1), 39-45. doi: 10.1111/j.1574-6968.1985.tb01129.x

Dalsgaard, T., Stewart, F.J., Thamdrup, B., De Brabandere, L., Revsbech, N.P., Ulloa, O., Canfield, D.E., DeLong, E.F., 2014. Oxygen at nanomolar levels reversibly suppresses process rates and gene expression in anammox and denitrification in the

508 oxygen minimum zone off northern Chile. Mbio. 5(6). doi: 10.1128/mBio.01966-14
509 de Matos, L.P., Costa, P.F., Moreira, M., Gomes, P.C.S., de Queiroz Silva, S., Gurgel, L.V.A.,
510 Teixeira, M.C., 2018. Simultaneous removal of sulfate and arsenic using immobilized
511 non-traditional SRB mixed culture and alternative low-cost carbon sources. Chem.
512 Eng. J. 334, 1630-1641. doi: 10.1016/j.cej.2017.11.035
513 Dev, S., Galey, M., Chun, C.L., Novotny, C., Ghosh, T., Aggarwal, S., 2021. Enrichment of
514 psychrophilic and acidophilic sulfate-reducing bacterial consortia-a solution toward
515 acid mine drainage treatment in cold regions. Environ Sci Process Impacts. 23(12),
516 2007-2020. doi: 10.1039/d1em00256b
517 Fei, X.F., Christakos, G., Xiao, R., Ren, Z.Q., Liu, Y., Lv, X.N., 2019. Improved heavy metal
518 mapping and pollution source apportionment in Shanghai City soils using auxiliary
519 information. Sci. Total Environ. 661, 168-177. doi: 10.1016/j.scitotenv.2019.01.149
520 Feng, S.S., Li, K.J., Huang, Z.Z., Tong, Y.J., Yang, H.L., 2019. Specific mechanism of
521 *Acidithiobacillus caldus* extracellular polymeric substances in the bioleaching of
522 copper-bearing sulfide ore. Plos One. 14(4). doi: 10.1371/journal.pone.0213945
523 Feng, X.N., Liu, Q.Y., Wang, S., Cen, L., Li, H.P., 2021. Arsenopyrite weathering in acid rain:
524 Arsenic transfer and environmental implications. J. Hazard. Mater. 420, 126612. doi:
525 10.1016/j.jhazmat.2021.126612
526 Fourçans, A., Ranchou-Peyruse, A., Caumette, P., Duran, R., 2007. Molecular analysis of the
527 spatio-temporal distribution of sulfate-reducing bacteria (SRB) in Camargue (France)
528 hypersaline microbial mat. Microb. Ecol. 56(1), 90-100. doi:
529 10.1007/s00248-007-9327-x
530 Fournier, M., Dermoun, Z., Durand, M.C., Dolla, A., 2004. A new function of the
531 *Desulfovibrio vulgaris* Hildenborough [Fe] hydrogenase in the protection against
532 oxidative stress. J. Biol. Chem. 279(3), 1787-1793. doi: 10.1074/jbc.M307965200
533 Giloteaux, L., Duran, R., Casiot, C., Bruneel, O., Elbaz-Poulichet, F., Goñi-Urriza, M., 2013.
534 Three-year survey of sulfate-reducing bacteria community structure in Carnoulès acid
535 mine drainage (France), highly contaminated by arsenic. FEMS Microbiol. Ecol.
536 83(3), 724-737. doi: 10.1111/1574-6941.12028
537 Gu, W.Z., Zheng, D.C., Li, D.P., Wei, C.C., Wang, X., Yang, Q.Z.M., Tian, C., Cui, M.Y.,

2021. Integrative effect of citrate on Cr(VI) and total Cr removal using a sulfate-reducing bacteria consortium. Chemosphere. 279, 130437. doi: 10.1016/j.chemosphere.2021.130437

Hwang, S.K., Jho, E.H., 2018. Heavy metal and sulfate removal from sulfate-rich synthetic mine drainages using sulfate reducing bacteria. Sci. Total Environ. 635, 1308-1316. doi: 10.1016/j.scitotenv.2018.04.231

Jenney, F.E., Verhagen, M.F.J.M., Cui, X.Y., Adams, M.W.W., 1999. Anaerobic microbes: Oxygen detoxification without superoxide dismutase. Science. 286, 306-309. doi: 10.1126/science.286.5438.30

Jia, T.P., Zhang, L., Zhao, Q., Peng, Y.Z., 2022. The effect of biofilm growth on the sulfur oxidation pathway and the synergy of microorganisms in desulfurization reactors under different pH conditions. J. Hazard. Mater. 432, 128638. doi: 10.1016/j.jhazmat.2022.128638

Jin, Q.S., Kirk, M.F., 2018. pH as a primary control in environmental microbiology: 1. Thermodynamic perspective. Front. Environ. Sci. 6. doi: 10.3389/fenvs.2018.00021

Kieu, H.T.Q., Müller, E., Horn, H., 2011. Heavy metal removal in anaerobic semi-continuous stirred tank reactors by a consortium of sulfate-reducing bacteria. Water Res. 45(13), 3863-3870. doi: 10.1016/j.watres.2011.04.043

Li, H., Yao, J., Min, N., Chen, Z.H., Li, M.M., Pang, W.C., Liu, B., Cao, Y., Men, D.Y., Duran, R., 2022a. Comprehensive evaluation of metal(loid)s pollution risk and microbial activity characteristics in non-ferrous metal smelting contaminated site. J. Clean. Prod. 344. doi: 10.1016/j.jclepro.2022.130999

Li, M.M., Yao, J., Sunahara, G., Duran, R., Liu, B., Cao, Y., Li, H., Pang, W.C., Liu, H.Q., Jiang, S., Zhu, J.J., Zhang, Q.H., 2023. Assembly processes of bacterial and fungal communities in metal(loid)s smelter soil. J. Hazard. Mater. 451, 131153. doi: 10.1016/j.jhazmat.2023.131153

Li, M.M., Yao, J., Sunahara, G., Hawari, J., Duran, R., Liu, J.L., Liu, B., Cao, Y., Pang, W.C., Li, H., Li, Y.Q., Ruan, Z.Y., 2022b. Novel microbial consortia facilitate metalliferous immobilization in non-ferrous metal(loid)s contaminated smelter soil: Efficiency and mechanisms. Environ. Pollut. 313, 120042. doi: 10.1016/j.envpol.2022.120042

Li, P.Z., Lin, C.Y., Cheng, H.G., Duan, X.L., Lei, K., 2015. Contamination and health risks of soil heavy metals around a lead/zinc smelter in southwestern China. Ecotoxicol. Environ. Saf. 113, 391-9. doi: 10.1016/j.ecoenv.2014.12.025

Li, Y., Dong, C.L., Li, Y., Nie, W.Q., Wang, M.W., Sun, C., Liang, L.F., Zhao, Z.Q., Zhang, Y.B., 2022c. Independent of direct interspecies electron transfer: Magnetite-mediated sulphur cycle for anaerobic degradation of benzoate under low-concentration sulphate conditions. J. Hazard. Mater. 423. doi: 10.1016/j.jhazmat.2021.127051

Liu, B.L., Ai, S.W., Zhang, W.Y., Huang, D.J., Zhang, Y.M., 2017. Assessment of the bioavailability, bioaccessibility and transfer of heavy metals in the soil-grain-human systems near a mining and smelting area in NW China. Sci. Total Environ. 609, 822-829. doi: 10.1016/j.scitotenv.2017.07.215

Liu, F.J., Zhang, G.P., Liu, S.R., Fu, Z.P., Chen, J.J., Ma, C., 2018. Bioremoval of arsenic and antimony from wastewater by a mixed culture of sulfate-reducing bacteria using lactate and ethanol as carbon sources. Int. Biodeter. Biodegr. 126, 152-159. doi: 10.1016/j.ibiod.2017.10.011

Liu, Y., Serrano, A., Wyman, V., Marcellin, E., Southam, G., Vaughan, J., Villa-Gomez, D., 2021. Nickel complexation as an innovative approach for nickel-cobalt selective recovery using sulfate-reducing bacteria. J. Hazard. Mater. 402. doi: 10.1016/j.jhazmat.2020.123506

Lv, Y., Zhu, X.Y., Zhang, M.J., Liu, X.Y., Wang, J.L., 2022. In-situ bioremediation of multiple heavy metals contaminated farmland soil by sulfate-reducing bacteria. Pol. J. Environ. Stud. 31(2), 1747-1755. doi: 10.15244/pjoes/141326

More, T.T., Yadav, J.S.S., Yan, S., Tyagi, R.D., Surampalli, R.Y., 2014. Extracellular polymeric substances of bacteria and their potential environmental applications. J. Environ. Manage. 144, 1-25. doi: 10.1016/j.jenvman.2014.05.010

Morris, J.G. 1975. The physiology of obligate anaerobiosis. Adv. Microb. Physiol, 169-246. doi: 10.1016/s0065-2911(08)60282-9

Nagar, S., Talwar, C., Motelica-Heino, M., Richnow, H.H., Shakarad, M., Lal, R., Negi, R.K., 2022. Microbial ecology of sulfur biogeochemical cycling at a mesothermal hot spring atop northern Himalayas, India. Front. Microbiol. 13. doi:

598 10.3389/fmicb.2022.848010
599 Nguyen, D., Wu, Z.Y., Shrestha, S., Lee, P.H., Raskin, L., Khanal, S.K., 2019. Intermittent
600 micro-aeration: New strategy to control volatile fatty acid accumulation in high
601 organic loading anaerobic digestion. Water Res. 166. doi:
602 10.1016/j.watres.2019.115080
603 Okabe, S., Ye, S.Y., Lan, X., Nukada, K., Zhang, H.Z., Kobayashi, K., Oshiki, M., 2023.
604 Oxygen tolerance and detoxification mechanisms of highly enriched planktonic
605 anaerobic ammonium-oxidizing (anammox) bacteria. ISME Commun. 3(1). doi:
606 10.1038/s43705-023-00251-7
607 Oshiki, M., Satoh, H., Okabe, S., 2016. Ecology and physiology of anaerobic ammonium
608 oxidizing bacteria. Environ. Microbiol. 18(9), 2784-2796. doi:
609 10.1111/1462-2920.13134
610 Ramel, F., Amrani, A., Pieulle, L., Lamrabet, O., Voordouw, G., Seddiki, N., Brèthes, D.,
611 Company, M., Dolla, A., Brasseur, G., 2013. Membrane-bound oxygen reductases of
612 the anaerobic sulfate-reducing *Desulfovibrio vulgaris* Hildenborough: roles in oxygen
613 defence and electron link with periplasmic hydrogen oxidation. Microbiology.
614 159(Pt_12), 2663-2673. doi: 10.1099/mic.0.071282-0
615 Ramel, F., Brasseur, G., Pieulle, L., Valette, O., Hirschler-Réa, A., Fardeau, M.L., Dolla, A.,
616 2015. Growth of the obligate anaerobe *Desulfovibrio vulgaris* Hildenborough under
617 continuous low oxygen concentration sparging: Impact of the membrane-bound
618 oxygen reductases. Plos One. 10(4). doi: 10.1371/journal.pone.0123455
619 Ran, H.Z., Guo, Z.H., Yi, L.W., Xiao, X.Y., Zhang, L., Hu, Z.H., Li, C.Z., Zhang, Y.X., 2021.
620 Pollution characteristics and source identification of soil metal(loid)s at an abandoned
621 arsenic-containing mine, China. J. Hazard. Mater. 413. doi:
622 10.1016/j.jhazmat.2021.125382
623 Ravenschlag, K., Sahm, K., Knoblauch, C., Jørgensen, B.B., Amann, R., 2000. Community
624 structure, cellular rRNA content, and activity of sulfate-reducing bacteria in marine
625 arctic sediments. Appl. Environ. Microbiol. 66(8), 3592-3602. doi:
626 10.1128/AEM.66.8.3592-3602.2000
627 Risatti, J.B., Capman, W.C., Stahl, D.A., 1994. Community structure of a microbial mat: the

phylogenetic dimension. Proc. Natl. Acad. Sci. USA. 91(21), 10173-10177. doi: 10.1073/pnas.91.21.10173

Rogers, K.L., Carreres-Calabuig, J.A., Gorokhova, E., Posth, N.R., 2020. Micro-by-micro interactions: How microorganisms influence the fate of marine microplastics. Limnol. Oceanogr. 5(1), 18-36. doi: 10.1002/lol2.10136

Rolfe, R.D., Hentges, D.J., Campbell, B.J., Barrett, J.T., 1978. Factors related to the oxygen tolerance of anaerobic bacteria. Appl. Environ. Microbiol. 36, 306-313. doi: 10.1128/aem.36.2.306-313.1978

Shi, J.X., Zhang, B.G., Cheng, Y.T., Peng, K.J., 2020. Microbial vanadate reduction coupled to co-metabolic phenanthrene biodegradation in groundwater. Water Res. 186, 116354. doi: 10.1016/j.watres.2020.116354

Si, S.C., Ke, Y.X., Xue, B.Q., Zhang, Z.Y., Zhu, X.L., 2023. Immobilized sulfate reducing bacteria (SRB) enhanced passivation performance of biochar for Zn. Sci. Total Environ. 892. doi: 10.1016/j.scitotenv.2023.164556

Sigalevich, P., Baev, M.V., Teske, A., Cohen, Y., 2000. Sulfate reduction and possible aerobic metabolism of the sulfate-reducing bacterium *Desulfovibrio oxyclinae* in a chemostat coculture with *Marinobacter* sp. strain MB under exposure to increasing oxygen concentrations. Appl. Environ. Microbiol. 66(11), 5013 - 5018. doi: 10.1128/AEM.66.11.5013-5018.2000

Sun, W.M., Xiao, E.Z., Xiao, T.F., Krumins, V., Wang, Q., Häggblom, M., Dong, Y.R., Tang, S., Hu, M., Li, B.Q., Xia, B.Q., Liu, W., 2017. Response of soil microbial communities to elevated antimony and arsenic contamination indicates the relationship between the innate microbiota and contaminant fractions. Environ. Sci. Technol. 51(16), 9165-9175. doi: 10.1021/acs.est.7b00294

Tally, F.P., Goldin, B.R., Jacobus, N.V., Gorbach, S.L., 1977. Superoxide dismutase in anaerobic bacteria of clinical significance. Infect. Immun. 16(1), 20-25. doi: 10.1128/iai.16.1.20-25.1977

Vita, N., Hatchikian, E.C., Nouailler, M., Dolla, A., Pieulle, L., 2008. Disulfide bond-dependent mechanism of protection against oxidative stress in pyruvate-ferredoxin oxidoreductase of anaerobic *Desulfovibrio* bacteria. Biochemistry.

47(3), 957–964. doi: 10.1021/bi7014713

Wang, J., Li, Q., Li, M.M., Chen, T.H., Zhou, Y.F., Yue, Z.B., 2014. Competitive adsorption of heavy metal by extracellular polymeric substances (EPS) extracted from sulfate reducing bacteria. Bioresour. Technol. 163, 374-376. doi: 10.1016/j.biortech.2014.04.073

Wang, Z.L., Zhang, B.G., He, C., Shi, J.X., Wu, M.X., Guo, J.H., 2021. Sulfur-based mixotrophic vanadium (V) bio-reduction towards lower organic requirement and sulfate accumulation. Water Res. 189, 116655. doi: 10.1016/j.watres.2020.116655

Wu, Z.T., Chen, Z.Y., Huang, W.H., Wei, Z.S., 2023. Flue gas arsenic trioxide removal from sludge incineration by sulfate-reducing membrane biofilm reactor. Fuel. 346. doi: 10.1016/j.fuel.2023.128295

Xiao, R., Guo, D., Ali, A., Mi, S.S., Liu, T., Ren, C.Y., Li, R.H., Zhang, Z.Q., 2019. Accumulation, ecological-health risks assessment, and source apportionment of heavy metals in paddy soils: A case study in Hanzhong, Shaanxi, China. Environ. Pollut. 248, 349-357. doi: 10.1016/j.envpol.2019.02.045

Xu, C.F., Su, X., Wang, J.H., Zhang, F.Z., Shen, G.N., Yuan, Y., Yan, L., Tang, H.Z., Song, F.Q., Wang, W.D., 2021a. Characteristics and functional bacteria in a microbial consortium for rice straw lignin-degrading. Bioresour. Technol. 331, 125066. doi: 10.1016/j.biortech.2021.125066

Xu, D.M., Fu, R.B., 2022. Mechanistic insight into the release behavior of arsenic (As) based on its geochemical fractions in the contaminated soils around lead/zinc (Pb/Zn) smelters. J. Clean. Prod. 363. doi: 10.1016/j.jclepro.2022.132348

Xu, D.M., Fu, R.B., Liu, H.Q., Guo, X.P., 2021b. Current knowledge from heavy metal pollution in Chinese smelter contaminated soils, health risk implications and associated remediation progress in recent decades: A critical review. J. Clean. Prod. 286. doi: 10.1016/j.jclepro.2020.124989

Yan, J., Ye, W.Z., Liang, X.S., Wang, S.J., Xie, J.H., Zhong, K.Q., Bao, M., Yang, J.B., Wen, H.J., Li, S.G., Chen, Y.H., Gu, J.D., Zhang, H.G., 2020. Enhanced reduction of sulfate and chromium under sulfate-reducing condition by synergism between extracellular polymeric substances and graphene oxide. Environ. Res. 183. doi:

10.1016/j.envres.2020.109157

Yan, X., Guan, D.X., Li, J., Song, Y.X., Tao, H., Zhang, X.M., Ma, M., Ji, J.F., Zhao, W.C., 2023. Fate of Cd during mineral transformation by sulfate-reducing bacteria in clay-size fractions from soils with high geochemical background. J. Hazard. Mater. 459. doi: 10.1016/j.jhazmat.2023.132213

Yue, X., Yu, G.P., Lu, Y.Q., Liu, Z.H., Li, Q.H., Tang, J.L., Liu, J., 2018. Effect of dissolved oxygen on nitrogen removal and the microbial community of the completely autotrophic nitrogen removal over nitrite process in a submerged aerated biological filter. Bioresour. Technol. 254, 67-74. doi: 10.1016/j.biortech.2018.01.044

Yun, S.W., Baveye, P.C., Kim, D.H., Kang, D.H., Lee, S.Y., Kong, M.J., Park, C.G., Kim, H.D., Son, J., Yu, C., 2018. Analysis of metal(loid)s contamination and their continuous input in soils around a zinc smelter: development of methodology and a case study in south Korea. Environ. Pollut. 238, 140-149. doi: 10.1016/j.envpol.2018.03.020

Zampieri, B.D.B., Nogueira, E.W., de Oliveira, A.J.F.C., Sanchez-Andrea, I., Brucha, G., 2021. Effects of metals on activity and community of sulfate-reducing bacterial enrichments and the discovery of a new heavy metal-resistant SRB from Santos Port sediment (Sao Paulo, Brazil). Environ. Sci. Pollut. Res. doi: 10.1007/s11356-021-15418-9

Zhang, B.G., Cheng, Y.T., Shi, J.X., Xing, X., Zhu, Y.L., Xu, N., Xia, J.X., Borthwick, A.G.L., 2019. Insights into interactions between vanadium (V) bio-reduction and pentachlorophenol dechlorination in synthetic groundwater. Chem. Eng. J. 375. doi: 10.1016/j.cej.2019.121965

Zhang, H.W., Zhang, F., Song, J., Tan, M.L., Kung, H.T., Johnson, V.C., 2021. Pollutant source, ecological and human health risks assessment of heavy metals in soils from coal mining areas in Xinjiang, China. Environ. Res. 202. doi: 10.1016/j.envres.2021.111702

Zhao, M.M., Zheng, G.G., Kang, X.Y., Zhang, X.Y., Guo, J.M., Zhang, M.X., Zhang, J.W., Chen, Y.P., Xue, L.G., 2023. Arsenic pollution remediation mechanism and preliminary application of arsenic-oxidizing bacteria isolated from industrial

718 wastewater. Environ. Pollut. 324. doi: 10.1016/j.envpol.2023.121384
719 Zhou, C., Vannela, R., Hayes, K.F., Rittmann, B.E., 2014. Effect of growth conditions on
720 microbial activity and iron-sulfide production by *Desulfovibrio vulgaris*. J. Hazard.
721 Mater. 272, 28-35. doi: 10.1016/j.jhazmat.2014.02.046
722 Zhou, J.M., Xing, J.M., 2021. Haloalkaliphilic denitrifiers-dependent sulfate-reducing
723 bacteria thrive in nitrate-enriched environments. Water Res. 201. doi:
724 10.1016/j.watres.2021.117354
725
726

## Figure captions

**Fig. 1.** Time course of pH and ORP (A), $OD_{600}$, and total As (B), and $SO_4^{2-}$ and $S^{2-}$ concentrations (C) during 7 d of the $As^{3+}$ immobilization of SRB1 consortium under anaerobic, anoxic, and aerobic conditions. Data are expressed as mean ± SD (n = 3).

**Fig. 2.** Scanning electron microscope images of metal precipitates formed during a 7-d biosynthesis process by SRB1 consortium under anaerobic (left column), anoxic (middle column), and aerobic (right column) conditions.

**Fig. 3.** X-ray diffraction patterns of metal precipitates formed during a 7-d biosynthesis process by SRB1 under anaerobic, anoxic, and aerobic conditions.

**Fig. 4.** XPS spectra of (A-C) As, (D-F) S, and (G-I) Fe species during 7 d of the $As^{3+}$ immobilization of SRB1 consortium under anaerobic (panels A, D, and G), anoxic (B, E, and H), and aerobic (C, F, and I) conditions.

**Fig. 5.** The compositions (A) and top 15 abundant genera (B) of the bacterial community of the SRB1 consortium under anaerobic, anoxic, and aerobic conditions. Treatment group letters: CK represents the initial inoculum, A, B, and C represent the anaerobic, anoxic, and aerobic conditions, respectively. Different lowercase letters in the boxplots indicate significant differences ($P < 0.05$) among different conditions.

**Fig. 6.** Co-occurrence patterns of SRB1 consortium. (A) At the phylum level, all the OTUs were kept, (B) while at the genus level. Only those genera with the sum of relative abundances > 0.005 were kept and the OTUs were filtered that simultaneously appeared in five samples. Edges are shown by strong correlations (Spearman $R > |0.7|$) and significant ($P < 0.05$). The nodes were colored by phylum level. The thickness of the edges corresponds to the strength of the correlation. Light pink lines indicate positive interactions and green lines indicate negative interactions. (C) FTIR spectra of EPS at day 7, and (D) the mean extracellular substance (EPS) content during 7 d of the $As^{3+}$ immobilization of SRB1 consortium under anaerobic, anoxic, and aerobic conditions. PS = polysaccharide, PN = extracellular protein, and HS = humic-like substances.

**Fig. 7.** A proposed model of $As^{3+}$ immobilization and survival strategy by SRB1 consortium under aerobic conditions.

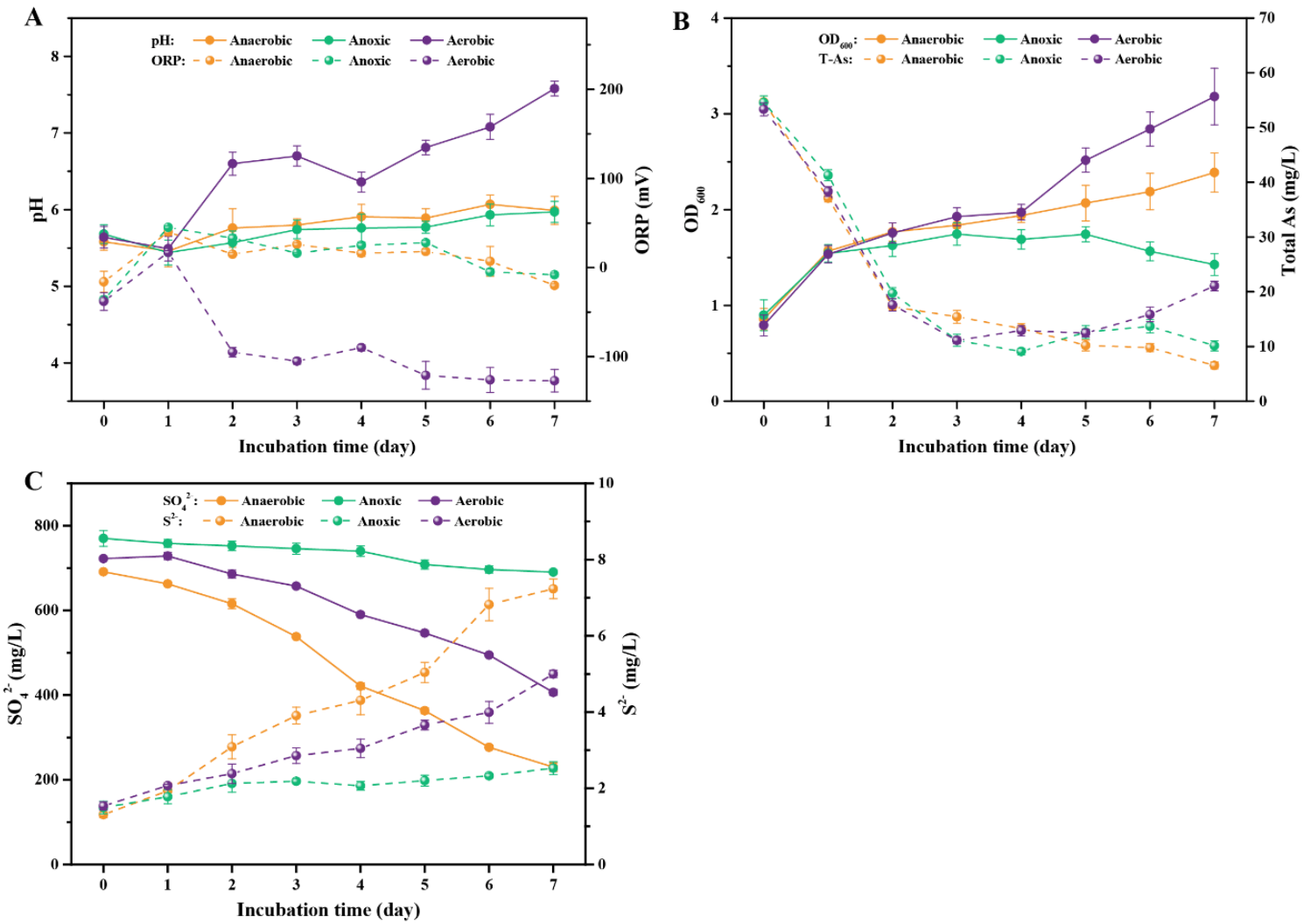


**Fig. 1.** Time course of pH and ORP (A), $OD_{600}$ and total As (B), and $SO_4^{2-}$ and $S^{2-}$ concentrations (C) during 7 d of the $As^{3+}$ immobilization of SRB1 consortium under anaerobic, anoxic, and aerobic conditions. Data are expressed as mean ± SD (n = 3).

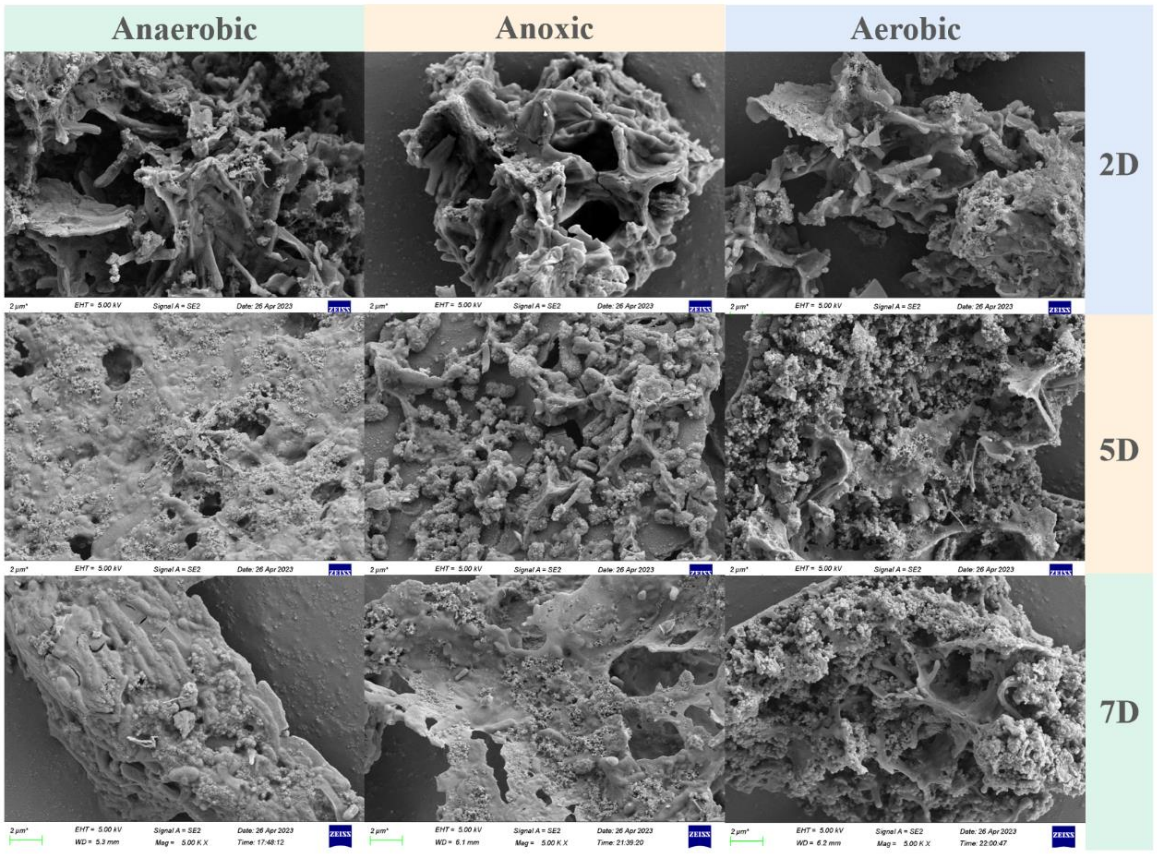


**Fig. 2.** Scanning electron microscope images of metal precipitates formed during a 7-d biosynthesis process by SRB1 consortium under anaerobic (left column), anoxic (middle column), and aerobic (right column) conditions.

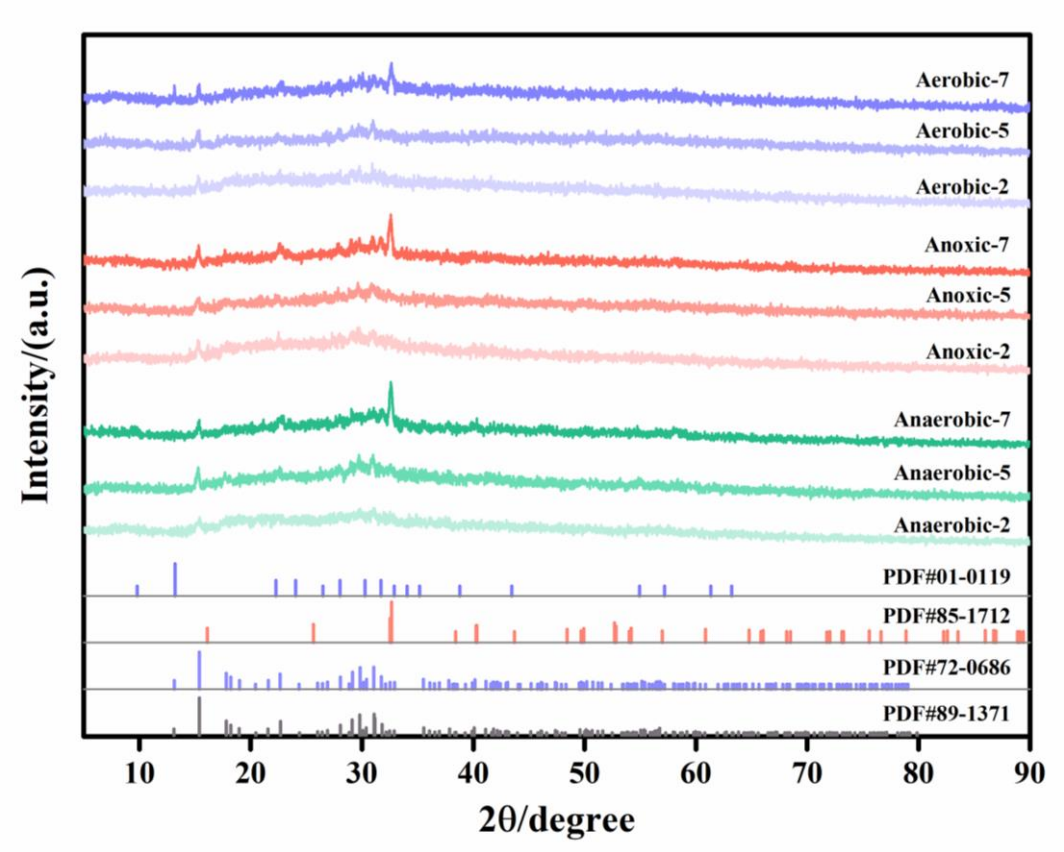


766

767 **Fig. 3.** X-ray diffraction patterns of metal precipitates formed during a 7-d biosynthesis

768 process by SRB1 under anaerobic, anoxic, and aerobic conditions.

769

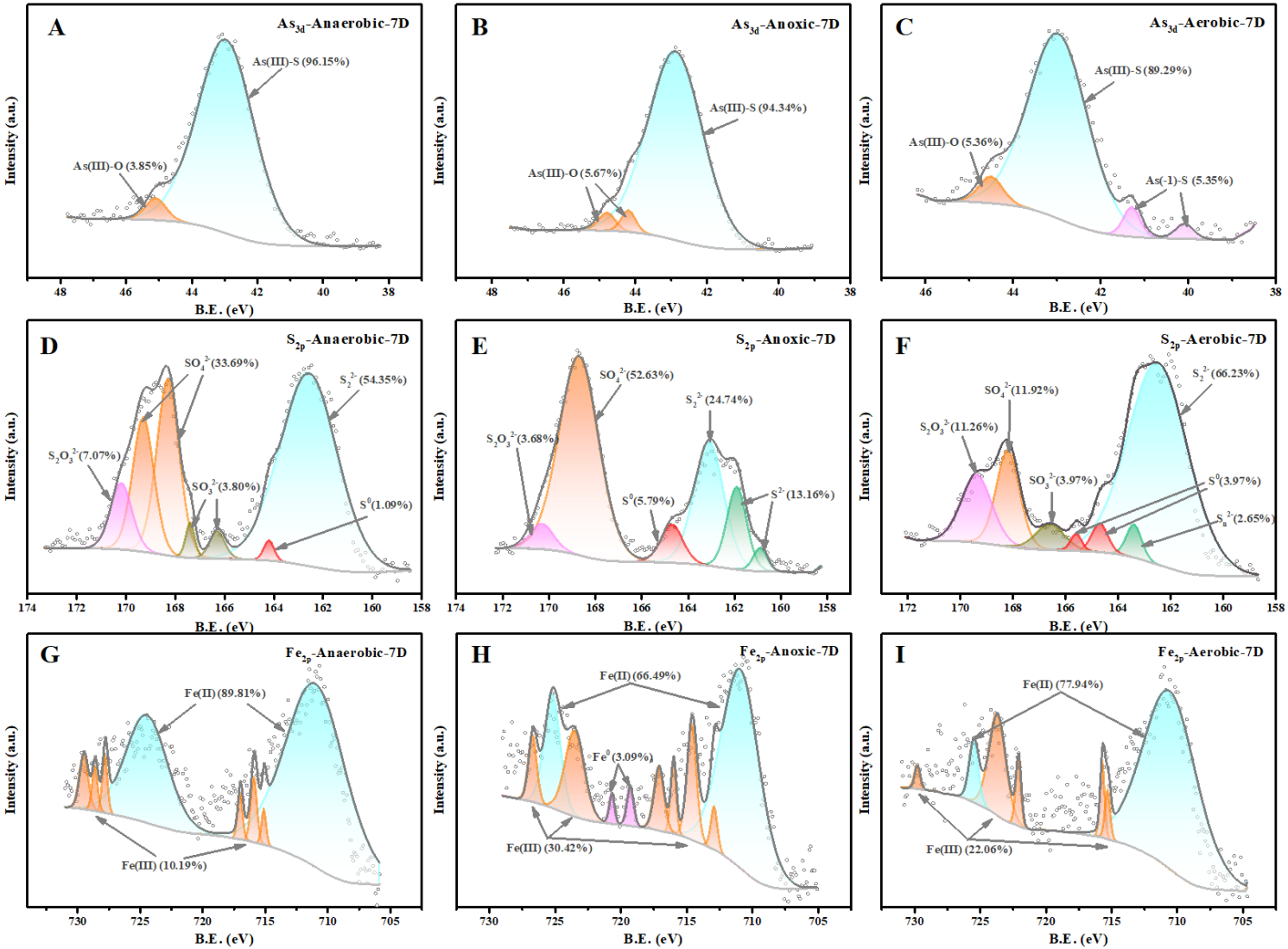


770

771 **Fig. 4.** XPS spectra of (A-C) As, (D-F) S, and (G-I) Fe species during 7 d of the $As^{3+}$ immobilization of SRB1 consortium under anaerobic

772 (panels A, D, and G), anoxic (B, E, and H), and aerobic (C, F, and I) conditions.

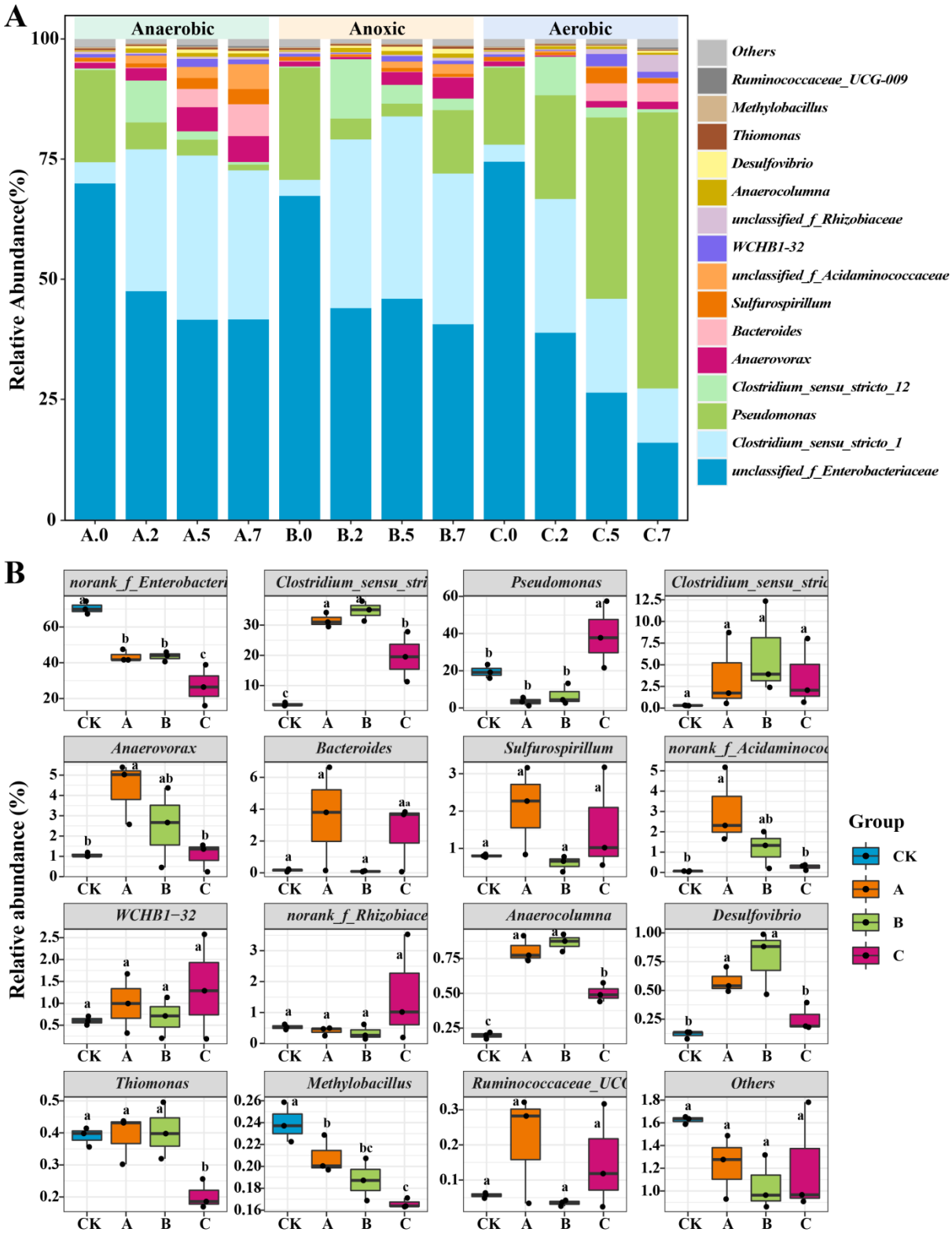


**Fig. 5.** The compositions (A) and top 15 abundant genera (B) of the bacterial community of the SRB1 consortium under anaerobic, anoxic, and aerobic conditions. Treatment group letters: CK represents the initial inoculum, A, B, and C represent the anaerobic, anoxic, and aerobic conditions, respectively. Different lowercase letters in the boxplots indicate significant differences ($P < 0.05$) among different conditions.

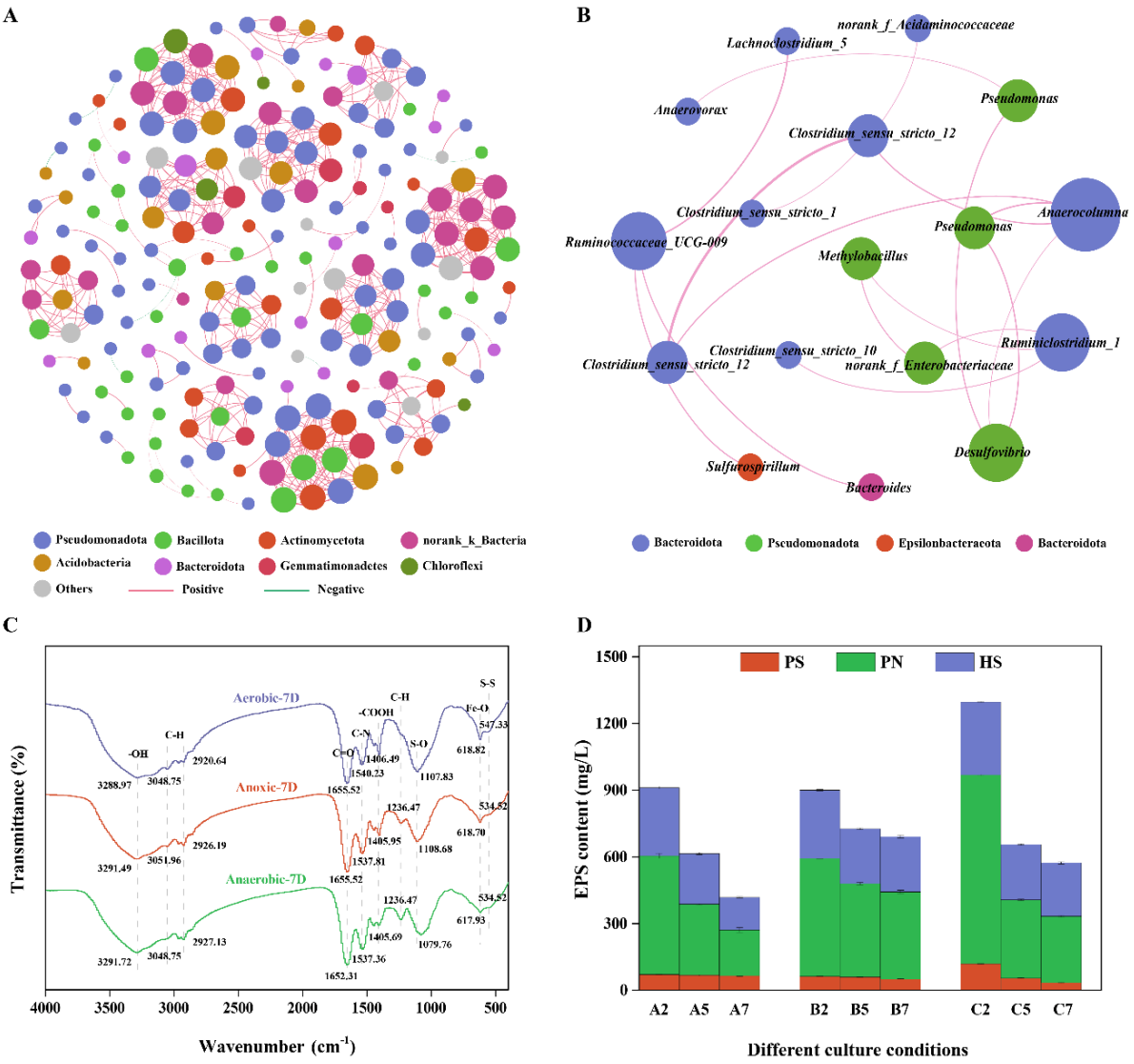


**Fig. 6.** Co-occurrence patterns of SRB1 consortium. (A) At the phylum level, all the OTUs were kept, (B) while at the genus level. Only those genera with the sum of relative abundances > 0.005 were kept and the OTUs were filtered that simultaneously appeared in five samples. Edges are shown by strong correlations (Spearman $R > |0.7|$) and significant ($P < 0.05$). The nodes were colored by phylum level. The thickness of the edges corresponds to the strength of the correlation. Light pink lines indicate positive interactions and green lines indicate negative interactions. (C) FTIR spectra of EPS at day 7, and (D) the mean extracellular substance (EPS) content during 7 d of the $As^{3+}$ immobilization of SRB1 consortium under anaerobic, anoxic, and aerobic conditions. PS = polysaccharide, PN = extracellular protein, and HS = humic-like substances.

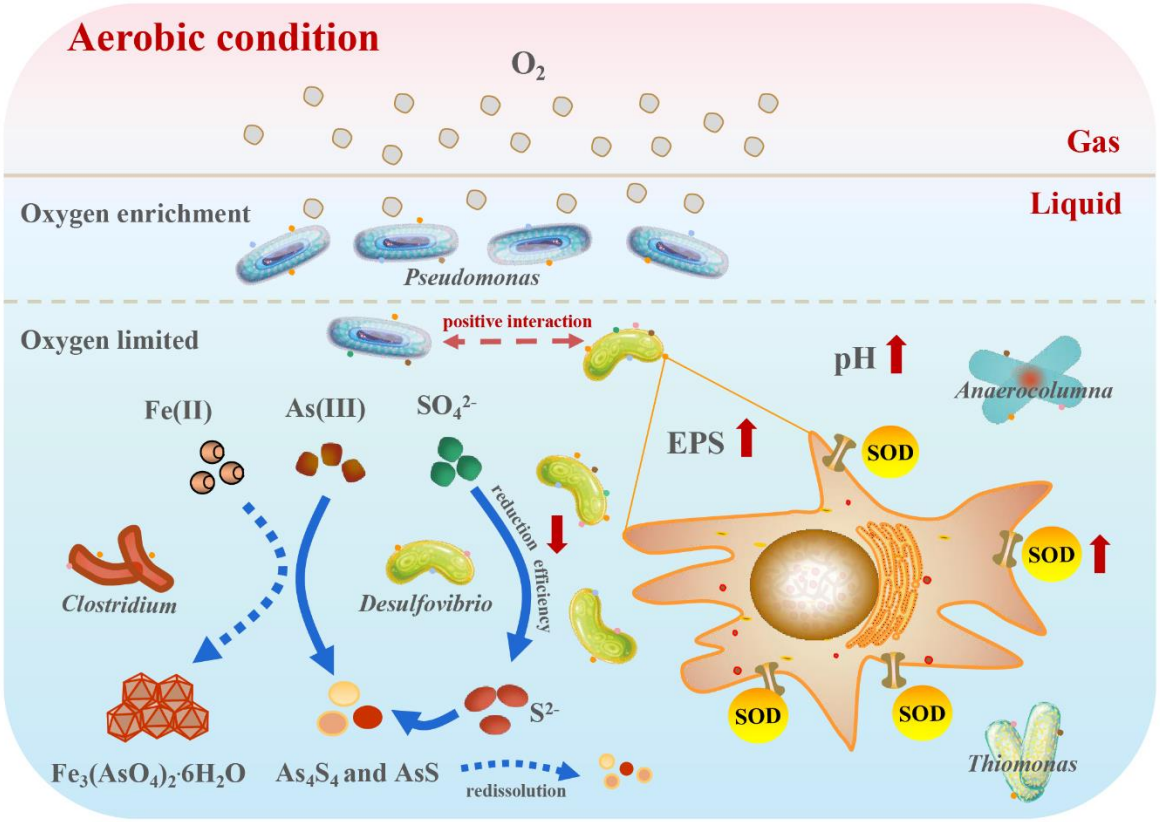


792

793 **Fig. 7.** A proposed model of $As^{3+}$ immobilization and survival strategy by SRB1 consortium

794 under aerobic conditions.